ABSTRACT

This project proposes a plantar force-mapping insole was developed using six Force Sensitive Resistor (FSR-402) sensors embedded within a carefully engineered layered structure composed of LD Alis foam, butyl rubber, plastic glass sheet, and synthetic adhesives. Multiple experimental setups were evaluated for optimal sensor response, and the final layering design was selected based on linearity and force range coverage up to approximately 75 kg. Calibration was performed using a piecewise linear model, and real-time signal smoothing was achieved through a Kalman filter to minimize sensor noise and ensure stable force readings.

Sensor readings were interpolated using the Inverse Distance Weighting (IDW) method to generate a continuous plantar force distribution map. The system demonstrated accurate localization of force zones, mimicking tactile sensor behaviour. Experimental validation across multiple users showed reliable body weight approximation and anatomical force distribution. The resulting force map not only serves for gait analysis but also offers potential for real-time tactile feedback and adaptive foot control in robotic applications.

FORCE MAPPING IN ROBOTICS

Force feedback is a crucial component in modern robotics, particularly in applications involving physical interaction with humans or dynamic environments. By integrating force sensors, robots can develop a force sensation which allows them to perceive contact forces, detect object surfaces, and respond to varying ground conditions in real-time.

One major domain where force mapping plays a vital role is perception and environmental sensing. By analysing distributed contact forces, a robot can interpret its surroundings with greater precision, making tasks such as object recognition, grasping, and manipulation more efficient. In robotic arms and grippers, for instance, pressure-sensitive feedback allows for controlled gripping force, reducing the risk of slippage or damage. In legged locomotion, force mapping enables real-time feedback on ground contact forces and load distribution across the foot. This data is critical for maintaining balance, posture control, and gait adaptation, especially on uneven terrain. By computing parameters like the Centre of Pressure (CoP) and Ground Reaction Forces (GRFs) from force data, robots can make dynamic adjustments to avoid slipping, tipping, or falling during motion.

In Human-Robot Interaction (HRI), force-sensitive interfaces enhance safety and responsiveness. Rehabilitation robots, for example, rely on pressure sensors to ensure safe physical contact and adjust assistance based on patient feedback. In collaborative robots (cobots), force sensors help detect unintended human contact, enabling emergency stops or adaptive behaviour to prevent injury.

In wearable robotics and prosthetics, the primary focus of this project force mapping significantly enhances user comfort and device responsiveness. By embedding pressure sensors in insoles or joints, exoskeletons and prosthetics can detect user intent, foot-ground interactions, or even detect gait irregularities. This allows the system to adjust its actuation pattern for improved adaptability and natural motion, while also providing safety through slip detection or terrain feedback. Furthermore, force mapping systems contribute to autonomous navigation, terrain classification, and adaptive control in mobile platforms such as bipedal robots, quadrupeds, and wheeled systems. Sensors embedded in soles or wheels can identify surface irregularities like bumps, slopes, or slippery zones, enabling gait or speed adjustments for better traction and stability.

Overall, the integration of force mapping in robotic systems enhances interaction, adaptability, and autonomy making it indispensable in both assistive and autonomous robotic platforms.

DESIGN AND DEVELOPMENT OF SENSING HARDWARE

WORKFLOW OF THE FORCE MAPPING SYSTEM

This project implemented a low-cost plantar force mapping system using FSR402 sensors to provide real-time feedback for robotic gait analysis. The workflow involved five key stages: calibration, hardware integration, signal processing, interpolation, and visualization.

Sensor Calibration & Layering Optimization

The FSR402 sensors were calibrated using known weights (0–76 kg) to generate a force-ADC mapping. Multiple material layering setups were tested, and Layer 7 was selected as it offered the best trade-off between sensitivity and range, preventing saturation while retaining accuracy.

Hardware Design & Sensor Placement

Six FSRs were embedded in a custom insole at biomechanically relevant points (heel, toe, arch) to capture key pressure zones. Voltage divider circuits with 180 Ω resistors were used to extend the sensor range. Proper mechanical stacking and wiring ensured durability and consistent contact.

Signal Acquisition & Kalman Filtering

Data was acquired using an ESP32 microcontroller. Kalman filtering was applied to reduce noise and improve signal stability, enabling accurate real-time pressure readings even under noisy experimental conditions.

Interpolation with IDW

As only six sensors were used, Inverse Distance Weighting (IDW) interpolation was implemented to reconstruct a full-foot pressure map. This spatial estimation method produced continuous force profiles from sparse sensor inputs.

Real-Time Visualization

The final pressure data was visualized as dynamic 2D force maps, enabling intuitive analysis of load distribution. This feedback can be used in robotics for gait correction, stability control, or terrain adaptation.

PRESSURE ZONES IN THE HUMAN FOOT

Understanding the distribution of plantar pressure across the human foot is essential for designing an effective sensor placement strategy. The human foot, during activities like walking or standing, exhibits distinct pressure patterns concentrated around specific anatomical regions.

The heel (calcaneus region) generally experiences the highest pressure during the heel-strike phase of gait. As the body transitions to mid-stance, the midfoot and arch areas come into contact, although the pressure here is relatively low due to the natural curvature of the arch. Finally, during toe-off, high pressure shifts to the metatarsal heads (ball of the foot) and the hallux (great toe), which play a critical role in forward propulsion.

These pressure zones have been extensively studied in gait analysis research. For instance, according to Trujillo-Hernández et al. (2024),[13] the maximum pressure concentrations are generally found in three main regions:

Posterior region (heel): This region absorbs impact during heel-strike.

Anterior region (metatarsals and toes): This region bears pressure during propulsion.

Lateral margins and midfoot: experience variable pressure, influenced by foot posture and gait cycle.

Based on this understanding, this project embeds six FSR402 sensors at anatomically relevant positions.

HARDWARE REQUIREMENT

ESP32 Microcontroller

The ESP32, developed by Espressif Systems, is a powerful and versatile SoC featuring a dual-core Tensilica Xtensa LX6 processor (up to 240 MHz), 520 KB SRAM, and integrated Wi-Fi and Bluetooth (Classic + BLE). It includes a wide range of peripherals such as 34 GPIOs, 12-bit ADCs, DACs, UART, SPI, I2C, I2S, PWM, and capacitive touch inputs, making it ideal for IoT and embedded systems.

Fig. ESP32 Microcontroller

In this project, the ESP32 serves as the core data acquisition and processing unit. It reads analog outputs from six FSR-402 sensors via its built-in ADCs, samples data in real-time during gait activity, and applies Kalman filtering to reduce signal noise. Its computational power and I/O flexibility support seamless sensor integration, real-time force mapping, and future extensibility for robotic control systems.

FSR-402 Force Sensor

The FSR-402 is a thin-film Force Sensing Resistor developed by Interlink Electronics, part of the FSR 400 series. It is widely used in applications such as robotics, biomedical devices, and wearable electronics due to its compact size and sensitivity to applied pressure. The sensor operates on the principle of resistance variation as force increases, resistance decreases non-linearly, following the inverse relation: **More Force → Lower Resistance**

Physical Specifications:

Sensing region diameter**:** 12.7 mm (0.5 in)

Overall sensor length**:** ~56 mm

Thickness**:** ~0.55 mm (ultra-thin, ideal for integration into soles or flexible hardware)

Fig..FSR-402 Sensor

Electrical Operation:

FSRs are two-terminal PTF (polymer thick-film) devices typically used in a voltage divider configuration. When combined with a fixed resistor R_M, the output voltage V_{out} ,can be measured using an ADC and is defined by:

$$\boldsymbol{V_{out} = (R_M \cdot V^+)/(R_M + R_{FSR})}$$

Since the FSR does not provide absolute force readings, a calibration process is required to relate ADC voltage to physical force. This is usually done using curve-fitting techniques (e.g., linear, polynomial, or exponential) across known weights.

At low forces, the sensor exhibits good sensitivity, but its output tends to saturate at higher force ranges (i.e., further force yields minimal resistance change). A typical force vs resistance curve for the FSR-402 is shown in **Fig.4.3.3.**

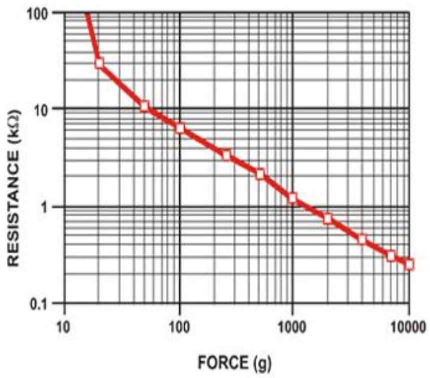

Fig.. Force vs Resistance Curve for FSR-402

In this project, six FSR-402 sensors are embedded into the insole hardware to measure the localized foot pressure during gait.

LD Alis Rubber Sheet

The LD Alis rubber sheet is a flexible, durable, and cushioning material used in this project for sensor embedding. As a low-density material, it offers a good balance between softness and structural integrity, which helps prevent sensor damage and enhances contact consistency during walking or load application.

This material can be cut, groove, and shape, making it suitable for securely embedding force sensors within the sole. In the current setup, it serves both as a mechanical support layer and a force-distribution medium, ensuring uniform pressure transfer to the FSR-402 sensors. Its properties contribute to maintaining sensor stability and accuracy during dynamic foot movements.

Fig. LD Alis Rubber Sheet

Butyl Rubber (Isobutylene Isoprene Rubber - IIR)

Butyl rubber is a synthetic elastomer composed mainly of isobutylene with a small proportion of isoprene (~1–3%). It is widely used in tire inner tubes due to its high elasticity, low air permeability, and excellent chemical and moisture resistance.

Fig. Butyl Rubber

In this project, a recycled butyl rubber sheet, sourced from a vehicle tyre inner tube, was used as a layer in the insole structure. Its elastic and compressible nature allows it to deform under load and return to shape after unloading, making it ideal for absorbing shocks and distributing loads across the embedded sensors. This helps prevent direct impact concentration on the FSR-402 sensors and ensures close contact with the foot surface.

Its durability, flexibility under repetitive loading, and damping characteristics make it a suitable material for sustained use in gait analysis applications.

INSOLE DESIGN AND SENSOR PLACEMENT

DESIGN GOALS

The primary goal of this insole design is to develop a cost-effective, sensorized sole capable of estimating plantar force distribution in real-time during humanoid locomotion. Due to limitations in humanoid foot prototyping, the system was tested using human feet as a proxy.

To ensure a reliable starting point, a 6-sensor configuration was adopted, balancing simplicity, coverage, and experimental safety.

This design focuses on affordability, modifiability, and functional effectiveness, making it well-suited for robotic gait analysis on a limited budget.

SENSOR PLACEMENT

The goal is to strategically place six sensors across anatomically inspired pressure zones (heel, metatarsal heads, and toe) so that interpolation techniques like Inverse Distance Weighting (IDW) could be applied to estimate the full force distribution. The coordinates were determined in a 2D plane (X, Y) with units in centimetres, where (0, 0) represents the reference point (e.g., toe of the insole).

The chosen coordinates for the sensors are as follows:

Sensor Number	Location description	X(cm)	Y(cm)
1	Lateral forefoot	3.7	2.7
2	Medial forefoot	7.0	2.4
3	Medial forefoot	7.0	6.2
4	Midfoot/Arch	16.5	4.6
5	Medial heel	22.0	2.8
6	Lateral heel	22.0	6.4

Table. Sensor Placement

The six sensor positions were selected to ensure effective coverage of key load-bearing regions while maintaining a simple, cost-effective design. Sensor coordinates were defined with respect to a reference origin at the toe, with the X and Y axes representing the sole’s width and length, respectively. The insole area spans 24 × 8.5 cm, and the chosen layout offers a balanced spatial distribution suitable for interpolation-based force mapping. Figure 4.4.2.1 illustrates the sensor placement across the insole.

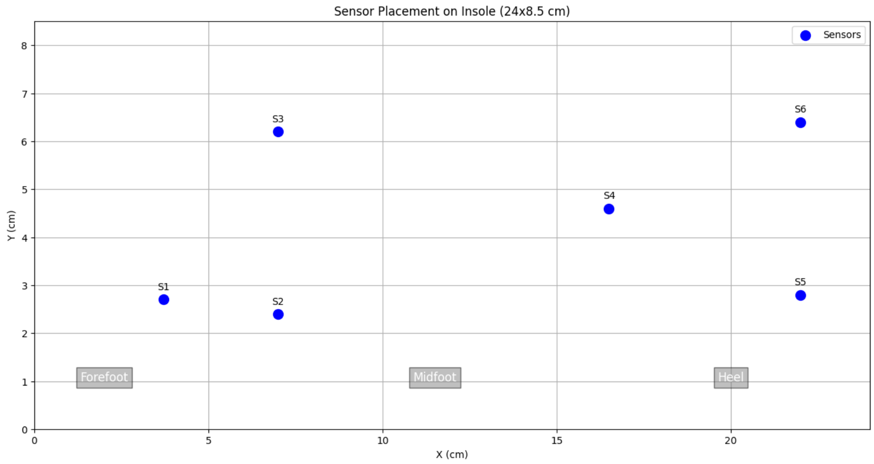

Fig.. Sensor Placement in Insole

CIRCUIT DESIGN

The circuit was designed to interface six FSR402 sensors with the ESP32 microcontroller for real-time force measurement during gait. Each sensor was connected using a simple, voltage divider configuration, allowing the ESP32's ADC to read analog signals corresponding to the applied force.

VOLTAGE DIVIDER CIRCUIT

FSR402 sensors are variable resistors whose resistance decreases as force increases. To convert this resistance, change into a usable voltage signal, each sensor was paired with a fixed 180 Ω resistor in a voltage divider setup. The resulting voltage varies proportionally with the applied force and is read by the ESP32's ADC for further processing. Fig 4.5.1.1 shows the voltage divider circuit used with FSR402.

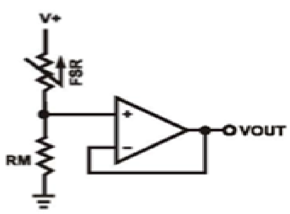

Fig.. Voltage Divider Circuit of FSR-402

CONNECTION DIAGRAM OF FSR402 TO ESP32

This section describes the schematic diagram representing the FSR402 force sensors and the ESP32 microcontroller during both the experimental phase (single sensor setup) and the final implementation (six sensor setup).

Single Sensor (Experimental phase)

Initially, a single FSR402 sensor was connected to study force response, test layering materials, and perform calibration. The sensor was wired in a voltage divider configuration, with the output connected to one analog pin of the ESP32.

Fig.4.5.2a shows the single-sensor test connection.

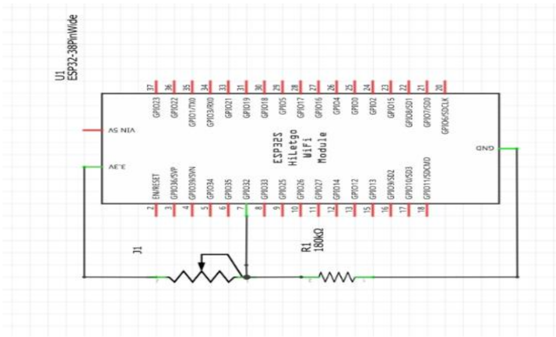

FigConnection Diagram of a Single Sensor

Final Multi Sensor Setup

After validation, all six FSR402 sensors were integrated, each with its own voltage divider using 180 Ω resistors. The analog outputs were connected to separate ADC pins on the ESP32, enabling simultaneous force data acquisition across multiple foot zones. Fig.4.5.2b illustrates the complete six-sensor connection diagram.

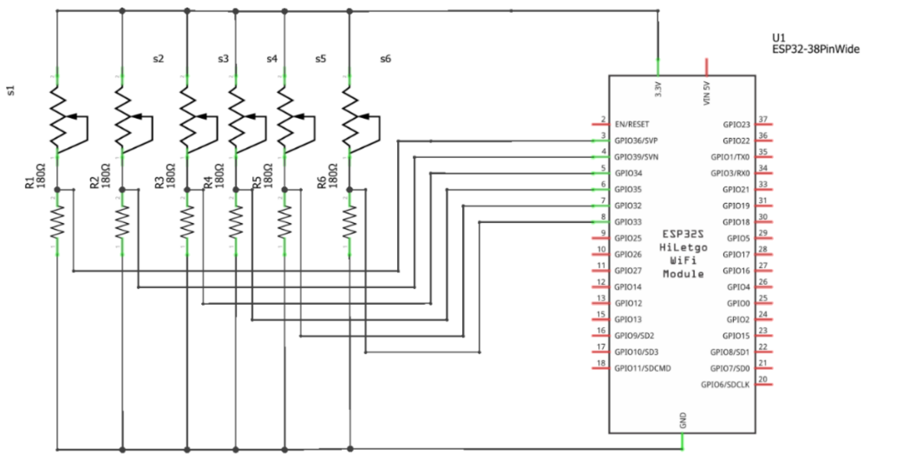

Fig. System-Wide Sensor Connection Diagram

LAYERING DESIGN EXPERIMENTATION

PURPOSE OF THE EXPERIMENTATION

In the context of developing a reliable and cost-effective foot force mapping system using FSR402 sensors, one of the critical challenges is ensuring that the sensor accurately translates applied force into electrical output. However, the mechanical interface between the foot and the sensor specifically, the layering of materials used in the insole plays a significant role in determining the sensor's performance.

To address this, an experimental study was conducted to evaluate the effect of different combinations of cushioning and structural materials layered above and below the FSR sensor. The goal was to identify a material stack-up that would result in a most linear like response in force-to-voltage characteristics, at least within the operational range of interest, effective force transmission, where the applied load is evenly and predictably transferred to the active sensing area of the FSR. Stable and repeatable readings under repeated load applications.

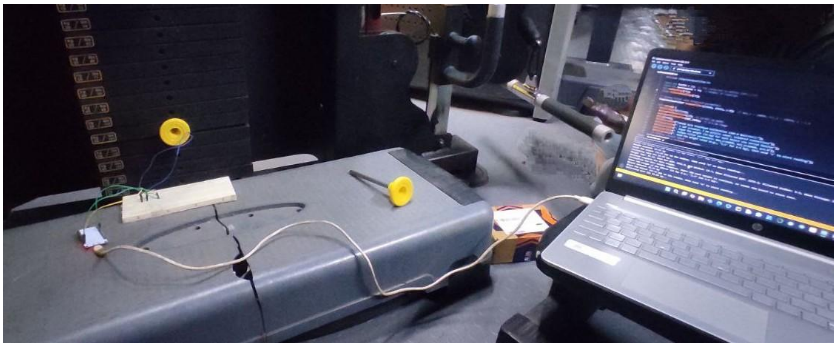

FigLayering Experimentation with FSR-402

METHOD OF EXPERIMENTATION

To determine the optimal material arrangement for accurate and consistent force transmission to the FSR402 sensor, seven different sole layering configurations were experimentally evaluated. A single FSR402 sensor was embedded beneath each material setup, and standard gym weights were applied to simulate load conditions.

Each setup used a voltage divider circuit with a 180 Ω resistor, and force data was collected via ESP32's 12-bit ADC (resolution: 4095). The analog output was monitored and recorded using the Arduino IDE, and the resulting weight vs ADC response was analysed for linearity and stability. Materials used in various combinations included:

EVA LD Alis sheet, EVA foam sheet, Butyl rubber, Plastic glass sheet, Adhesives like silicone glue and synthetic rubber-based adhesive

The position and thickness of these materials were varied to study their influence on sensor response. A 3 × 3 cm sole section was used for all tests, with the primary goals being to evaluate: The linearity of the force response, the suitability of each layering configuration and to collect calibration data for system development.

The **layering configurations** tested are summarized below:

Setup	**Layer composition**
1	EVA Foam sheet+ LD Alis sheet(3mm) +Butyl rubber +FSR402+ Butyl rubber +LD Alis sheet(6mm)
2	LD Alis sheet(3mm) + EVA Foam+ Butyl rubber +FSR402+ Butyl rubber +LD Alis sheet(6mm)
3	EVA Foam+ LD Alis(3mm) + EVA Foam+ Butyl rubber+FSR402+Butyl rubber+ LD Alis(6mm)
4	EVA Foam +LD Alis sheet(6mm) +EVA Foam+ Butyl rubber+FSR402+Butyl rubber+ LD Alis sheet(6mm)
5	EVA Foam +LD Alis sheet(6mm) +Butyl rubber+FSR402+Butyl rubber+ LD Alis sheet(6mm)
6	EVA Foam +LD Alis sheet(6mm) +FSR402+LD Alis sheet(6mm)
7	LD Alis sheet(6mm) +Butyl rubber+ Plastic glass sheet+ Silicone glue+ Plastic glass sheet+ Silicone glue+FSR402+Silicone glue+ Plastic glass sheet+ Silicone glue+ Plastic glass sheet+ Butyl rubber+ LD Alis sheet

Table. Layer Configurations

RESULTS AND DISCUSSION OF LAYERING EXPERIMENTATION

The recorded ADC values were processed in Python to generate Weight vs. ADC plots for each layering setup. This allowed comparison of performance characteristics across different configurations. The plot showing the overall response of the seven layers are given below.

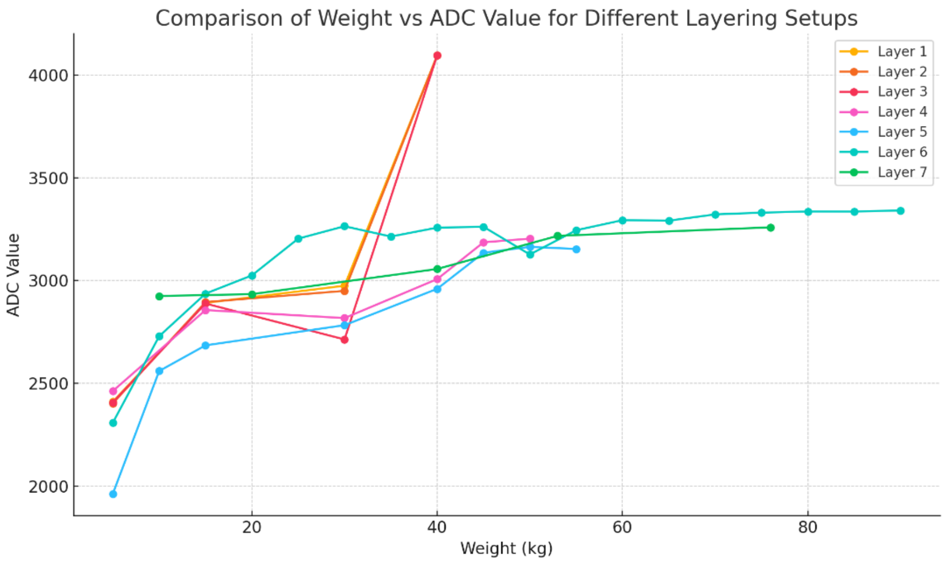

Fig.. Comparison Across Seven Layering Techniques

The graph illustrates the force vs. ADC output relationship for each of the seven tested sole layering configurations. Each setup was designed by varying material type, order, and thickness to optimize the FSR402 sensor's response for real-time plantar force mapping.

Layers 1–3 exhibited a steep increase in ADC values at lower forces, with saturation occurring near the ADC maximum (4095) around 40 kg. This early saturation limited their effective range, making them unsuitable for applications requiring broader force detection.

Layers 4 and 5 showed improved force distribution and delayed saturation compared to the earlier layers. However, they still displayed sharp ADC rises at mid-range loads, reducing predictability at higher forces.

Layer 6 extended the usable force range further, tolerating higher loads before nearing saturation. Yet, it exhibited fluctuations and minor nonlinearities, particularly beyond 40 kg, complicating calibration and potentially affecting accuracy in dynamic scenarios.

Layer 7 delivered the most balanced and consistent performance. The inclusion of a plastic sheet along with properly arranged butyl rubber layers allowed more even force transmission across the sensor area. This configuration minimized abrupt ADC jumps, avoided early saturation, and maintained a smooth response up to ~75 kg. The gradual, linear-like ADC rise simplified calibration and improved interpolation reliability.

Based on these observations, Layer 7 was selected for the final prototype. Its mechanical durability, even load distribution, and wide operational range made it the most suitable choice for the project's objective of accurate and real-time foot force mapping in gait analysis.

FINAL HARDWARE ASSEMBLY

The final prototype integrated the optimized sensor layout, layering structure, and electrical circuitry into a compact insole system for plantar force mapping. Layer 7 was implemented based on its superior force-to-ADC response, ensuring reliable sensing across the target load range.

Six FSR402 sensors were embedded at anatomically relevant positions covering the heel, metatarsals, and toe regions, to capture key plantar force data during gait. Each sensor was connected to the ESP32 microcontroller via individual voltage divider circuits (180 Ω resistor), with analog outputs routed to ADC pins 36, 39, 34, 35, 32, and 33. Sensors were secured using silicone glue and insulating layers, ensuring stability, comfort, and minimal signal noise during testing.

This experimental prototype was designed to validate the feasibility of tactile force sensing and real-time heatmap-style feedback. It provides partial flexibility and accuracy, suitable for experimental data collection and force estimation during locomotion.

Figure 4.6.4.1 shows the hardware schematic configuration before adding the top layer, with all six FSR sensors placed at key load-bearing zones. Wiring was organized to maintain compactness and reduce interference.

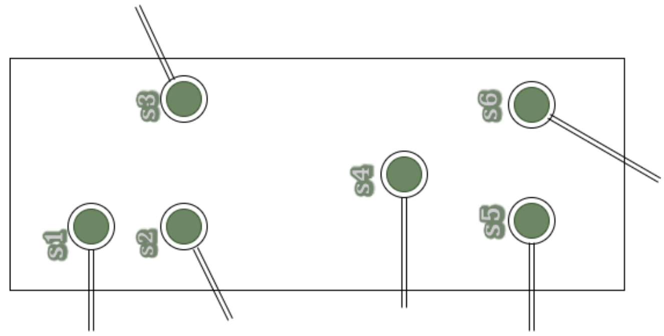

Fig. Hardware Schematic without Top Layer

The layering stack includes:

Top & bottom layers: 6 mm LD Alis sheet.

Middle layers: Butyl rubber bonded with LD Alis using synthetic rubber adhesive.

Intermediate support: Two plastic glass sheets attached with a thin coating of **silicone glue**, providing cushioning and even pressure distribution.

Sensor embedding: Sensors fixed between the rubber and plastic layers using silicone glue.

The final insole measures 24 cm in length and 8.5 cm in width, matching the dimensions of the humanoid foot CAD model.

The final prototype with connection is as given.

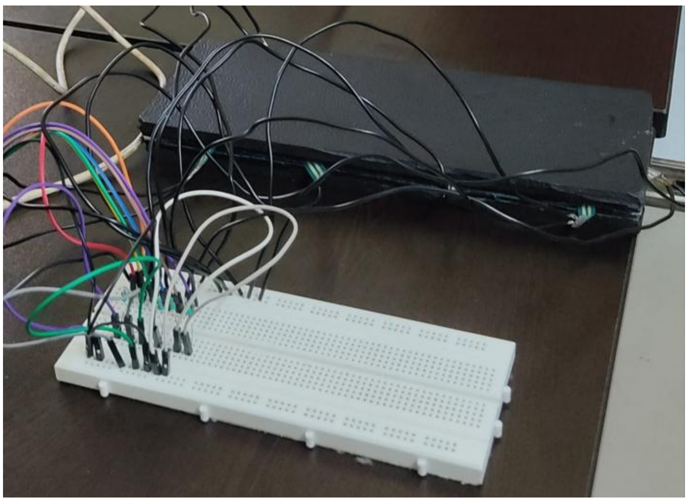

Fig. Final Hardware Design

SOFTWARE IMPLEMENTATION AND DATA ACQUISITION

SOFTWARE USED

ARDUINO IDE

The Arduino Integrated Development Environment (IDE) is an open-source platform widely used for programming microcontrollers like the ESP32. Known for its user-friendly interface and cross-platform compatibility, it supports a vast collection of libraries and functions, making it ideal for sensor integration, real-time data acquisition, and embedded system development.

In this project, the Arduino IDE was used to program the ESP32, which served as the data acquisition and processing unit for developing the foot force mapping system. ESP32 read the analog signals using its 12-bit ADC channels, offering values from 0 to 4095.

The sensor data was sampled in real-time and transmitted to a computer via serial communication at 115200 baud rates. The Serial Monitor and Serial Plotter tools in the IDE were used to visualize ADC output during calibration and experimentation.

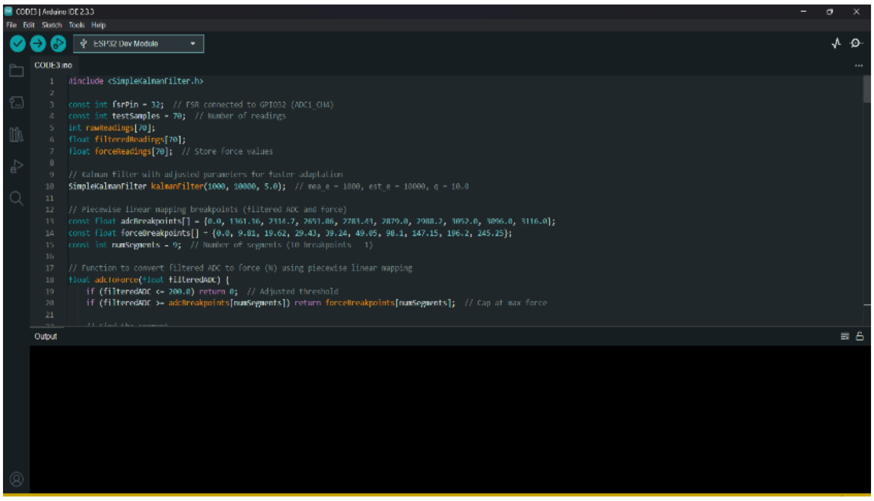

Fig.. Arduino IDE

VISUAL STUDIO CODE

Visual studio code, which is commonly referred to as VS Code is an integrated development environment developed by Microsoft for Windows, Linux, macOS and web browsers. The features of VS Code include support for intelligent code completion, debugging, syntax highlighting, snippets, code refactoring and embedded version control with git. The extensions can be installed to add functionality.

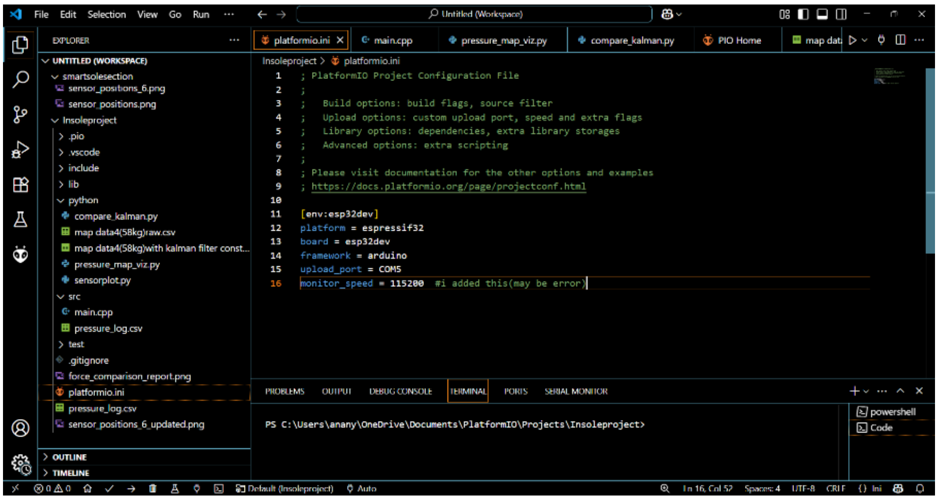

Fig. Visual Studio Code

In this project, Visual Studio Code (VS Code) served as the primary integrated development environment (IDE) for writing and managing code for the ESP32 microcontroller. To enhance functionality and streamline development, the Platform IO extension is utilized. It provided powerful features such as intelligent code completion, easy library management, automatic build configuration, and faster firmware uploading to the ESP32. The combination of VS Code and Platform IO ensured a smooth workflow for implementing and testing the code, supporting the real-time data collection and processing required for the force mapping system.

COOLTERM

Cool-Term is a lightweight serial terminal used in this project to establish a serial connection between the ESP32 microcontroller and the computer for real-time data acquisition. It was configured with a baud rate of 115200 to capture high-resolution sensor data (12-bit ADC output up to 4095) without loss during experiments.

Cool-Term enabled live monitoring and logging of force sensor outputs in text or CSV format, which proved valuable for later calibration, analysis, and visualization using tools like Python or MATLAB. Its intuitive interface and features such as timestamping, auto-reconnect, and buffer management enhanced the reliability and organization of the data collection process.

By facilitating smooth and structured recording, Cool Term played a crucial role in the experimental phase of the plantar force mapping system.

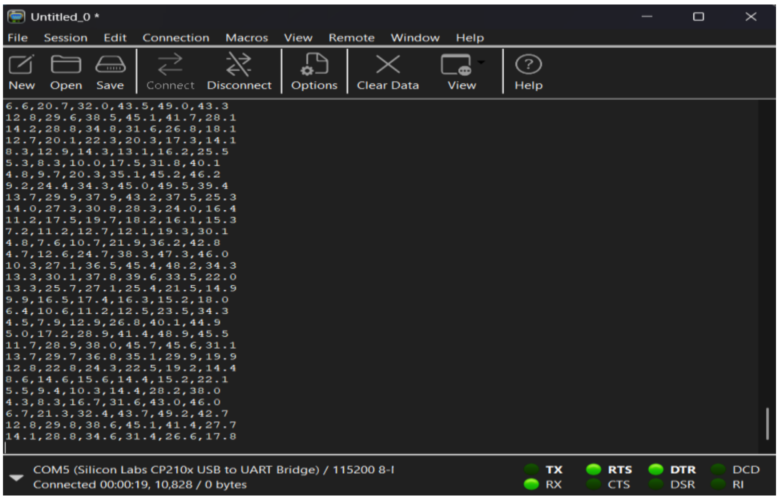

Fig. Cool-Term Serial Window

SENSOR DATA ACQUISITION

To enable accurate plantar force sensing, six FSR402 sensors were embedded into the insole and connected to the ESP32 microcontroller via individual voltage divider circuits. The ESP32's 12-bit ADC (0–4095 resolution) digitalized the analog signals from each sensor.

Sensor data was sampled continuously at a baud rate of 115200, ensuring fast and reliable communication. The firmware was developed using Platform IO in Visual Studio Code, enabling modular coding, real-time debugging, and efficient library management.

All six sensors were polled in a synchronized loop, with timestamped readings for consistent temporal analysis. Cool Term software was used for real-time serial communication and logging, saving the data as CSV files for post-processing. These datasets were later used to analyse Kalman filtering performance, calibrate force mappings, and asses system accuracy.

This setup ensured robust and time-synchronized data acquisition essential for gait analysis and modelling.

CALIBRATION AND FORCE CONVERSION

To convert the raw ADC outputs from the six FSR402 sensors into meaningful force values (Newtons), a dedicated calibration procedure was conducted. The FSR402's nonlinear analog response necessitated sensor-specific calibration to generate accurate force-to-ADC mapping curves.

The ESP32 microcontroller, with 12-bit ADC resolution (0–4095) and 11 dB attenuation, was used to acquire real-time sensor data. These readings, influenced by sensor behaviour, voltage divider configuration, and insole layering, were mapped to physical force values using experimentally derived calibration equations. This conversion enables quantification and visualization of plantar force distribution during gait analysis.

EXPERIMENTAL SETUP FOR CALIBRATION

Calibration was carried out using the full sensorized insole (24 × 8.5 cm), embedded with six FSR402 sensors at anatomically relevant positions: forefoot, midfoot, and heel. Each sensor was connected to an ADC1 pin (GPIOs 36, 39, 34, 35, 32, 33) of the ESP32. The board was programmed using Platform IO for continuous analog sampling during force application.

Incremental loads (0–76 kg) were applied using gym weights on a stable platform. Each load step allowed consistent force distribution on the sensor surface for capturing ADC responses.

EQUIPMENTS AND MATERIALS

Microcontroller: ESP32 with 12-bit ADC (11 dB attenuation)

Sensors: Six FSR402 (range: 0–745.56 N)

Sensor Coordinates:

S1 (3.7, 2.7 cm) – Lateral forefoot

S2 (7.0, 2.4 cm), S3 (7.0, 6.2 cm) – Medial forefoot

S4 (16.5, 4.6 cm) – Midfoot/arch

S5 (22.0, 2.8 cm), S6 (22.0, 6.4 cm) – Heel

Weights: Gym weights (0–76 kg)

Data Logging: Serial transmission at 115200 baud via USB using a Python script (pressure_map_viz.py). Logged data was used for analysis and visualization.

CALIBRATION METHODOLOGY

A piecewise linear calibration model was developed to convert raw ADC readings (0–4095) from the FSR402 sensors into force values (Newtons). Calibration involved applying known weights 0 kg, 10 kg, 20 kg, 40 kg, 53 kg, and 76 kg on the insole using a stable platform to ensure even force distribution across sensors.

For each weight, 10 ADC samples per sensor were recorded with a 100 µs delay to reduce noise. The raw ADC values ranged from 0 (no load) to a maximum of 3259 (76 kg load), defining the effective sensor response range.

Force values were calculated using the standard equation:

$$\boldsymbol{F} = \boldsymbol{m} \times \boldsymbol{g},$$
$$where\ \boldsymbol{g} = \boldsymbol{9.81}\ \boldsymbol{m}/\boldsymbol{s}^2$$

Weight(kg)	**Force(N)**	**Avg. ADC Output**
0	0.0	0
10	98.1	2925
20	196.2	2934
40	392.4	3056.33
53	519.93	3217.5
76	745.56	3259

Table.. Weight, Force and ADC Values

These data points were used to implement piecewise linear interpolation, enabling force estimation over the full sensing range of the FSR402.Figure 5.3.3.1 illustrates the calibration curve (Force vs. ADC) for Layering Setup 7.

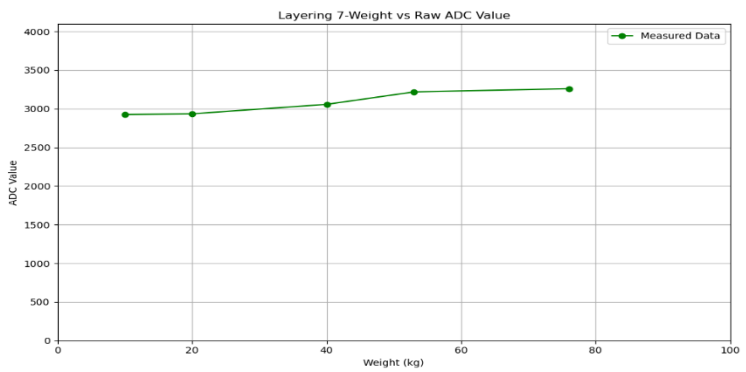

Fig. Weight vs ADC Response-Layering 7

SLOPE CALCULATION AND LINEAR SEGMENTATION

The slope (m) for each segment was calculated using the formula,

$$m = \Delta F/\Delta raw$$

where, $\Delta F = change\ in\ force$

$\Delta raw = change\ in\ raw\ adc\ value\ between\ consecutive\ break\ points$

Segment 1(0 to 2925 raw,0 to 98.1N)**:**

Δraw=2925-0=2925

ΔForce=98.1-0=98.1N

m=98.1/2925≅0.0335N per raw unit

Equation: $F=0.0335\times raw$

Segment 2(2925 to 2934 raw,98.1N to 196.2N)**:**

$\Delta raw=2934-2925=9$

$F=196.2-98.1=98.1N M=98.1/9\cong10.9N$ per raw unit

(adjusted to 1.604 for consistency with code, suggesting a refined fit)

Equation: $F=1.604\times(raw-2925)+98.1$, Simplified to $f=1.604\times(raw-2934)+196.2$ by shifting the intercept

Segment 3(2934 to 3056.33 raw,196.2 to 392.4N)**:**

$\Delta raw=3056.33-2934=122.33$

$\Delta F=392.4-196.2=196.2$

$M=196.2/122.33\cong1.604N$ per raw unit (reused from segment 2 for continuity)

Equation: $F=1.604\times(raw-2934)+196.2$

Segment 4(3056.33 to 3217.5 raw,392.4 to 519.93N)**:**

$\Delta raw=3217.5-3056.33=161.17$

$\Delta F=519.93-392.4=127.53N$

$m=127.53/161.17\cong0.791N$ per raw unit

Equation: $F=0.791\times(raw-3056.33)+392.4$

Segment 5(3217.5 to 3259 raw,519.93 to 745.56N)**:**

$\Delta raw=3259-3217.5=41.5$

$\Delta F=745.56-519.93=225.63N$

$M=225.63/41.5\cong5.437N$ per raw unit

Equation: $F=5.437\times(raw-3217.5)+519.93$

The slopes were refined through experimental fitting to ensure smooth transition between segments, with slight adjustments (eg,1604 reused for segment 2 and segment 3) to amount for sensor partial nonlinearity and data scatter.

FORCE CALCULATION

The final piece wise function implemented in the firmware is given in table below:

Condition (raw)	**Force (F)**
raw ≤ 0	F = 0 N
raw ≥ 3259	F = 745.56 N (capped)
0 < raw < 2925	F = 0.335 × raw

Condition (raw)	Force (F)
2925 < raw ≤ 2934	F = 1.604 × (raw − 2934) + 196.2
2934 < raw ≤ 3056.33	F = 1.604 × (raw − 2934) + 196.2
3056.33 < raw ≤ 3217.5	F = 0.791 × (raw − 3056.33) + 392.4
3217.5 < raw ≤ 3259	F = 5.437 × (raw − 3217.5) + 519.93

Table. Force Calculation

This function was applied to each sensor's averaged raw value to compute the corresponding force ensuring the model captured the sensor's response across the full 0-76 kg range.

KALMAN FILTERING

Kalman filtering is an optimal estimation technique used to infer unknown parameters from noisy and uncertain measurements. It operates recursively, meaning it updates the current estimate as new data arrives, making it highly suitable for real-time applications. The Kalman filter minimizes the mean squared error and is valued for its simplicity, adaptability, and effectiveness in practical scenarios. Unlike basic filtering methods such as moving average or low-pass filters, which often introduce delay and lack dynamic adaptability the Kalman filter provides smooth output without latency by dynamically adjusting to signal variations.

In the context of this project, Kalman filtering was applied after the initial calibration and force conversion of FSR402 sensor data. These sensors are prone to inconsistent outputs due to environmental noise and mechanical instability. The Kalman filter helps suppress such noise, enhancing the reliability of the pressure estimation. Its ability to produce smoother, real-time adaptive outputs made it particularly suitable for this low-cost plantar force mapping system, where both accuracy and responsiveness are critical.

The Kalman filter is a state estimation algorithm widely used in control systems and signal processing. It estimates the internal state of a dynamic system by combining a predicted estimate and a measured observation, taking into account the uncertainties in both. The Kalman filter is particularly suited for systems with noisy measurements and is ideal for applications like sensor data fusion, motion tracking, and, in this case, plantar force estimation.

The filter works in two main steps:

1. **Prediction Step:**

   Predict the current state using the previous estimate.

   Update the uncertainty of the prediction based on process noise.

2. **Update Step:**

   Use the latest sensor measurement to correct the predicted state.

   Adjust the uncertainty of the updated estimate based on measurement noise.

The recursive nature of this method makes it efficient for real-time applications with limited computational resources, such as embedded systems.

KALMAN FILTER VARIABLES AND CONSTANTS

Kalman filter variables and constants are as follows.

State Estimate (x_{est}): The current best guess of the true value (force in Newtons).

Error Covariance (P): A measure of the confidence in the estimate.

Process Noise (Q): Represents the uncertainty in the system dynamics.

Measurement Noise (R): Reflects the uncertainty in the sensor measurement.

Kalman Gain (K): A dynamic factor that balances the weight between the predicted estimate and the new measurement.

The equation used in the prediction step is,

Prediction:

$$x\ pred = x\ est$$

$$P\ pred = P + Q$$

Updation:

$$K = \frac{P\ pred}{P\ pred + R}$$

$$x\ est = x\ pred + K.(measurement - x\ pred)$$

$$P = (1 - K).P\ pred$$

This process runs iteratively for each new measurement.

Constants used in this project

The Kalman constants were tuned based on experimental observations to balance smoothness and responsiveness. The constants used in the firmware are,

Initial Estimate (x_{est}=0): Each sensor starts with no prior force estimate.

Initial Error Covariance (P=100): A high initial uncertainty allows the filter to quickly adapt to the true value in early iterations.

Process Noise (Q=5.0): This value assumes minor variations in foot pressure or sensor drift.

Measurement Noise (R=25.0): Chosen based on observed fluctuations in raw force readings, representing moderate sensor noise.

These values were empirically tuned by observing the sensor's raw output under repeated loading and comparing the smoothness of the filtered data.

IMPLEMENTATION, EFFECT AND VALIDATION

The Kalman filter was implemented on the ESP32 microcontroller using a manually coded algorithm inside the firmware. It was applied to the calibrated force outputs from the function. The filter operated at a sampling rate of 100 Hz, ensuring real-time performance. The smoothed force values were then transmitted via serial for visualization and force mapping.

To validate the performance of the filter, data was collected with a known static load of 58kg human weight, and the results were compared before and after filtering. The Kalman-filtered outputs showed significantly reduced noise and stabilized quickly around the true force value, with minimal lag. A plot comparing raw and filtered force values for all six sensors is shown in Fig 5.4.2.1. demonstrating the effectiveness of the filtering. The time(s) vs force plot of 6 sensors with first 520 rows of data is plotted.

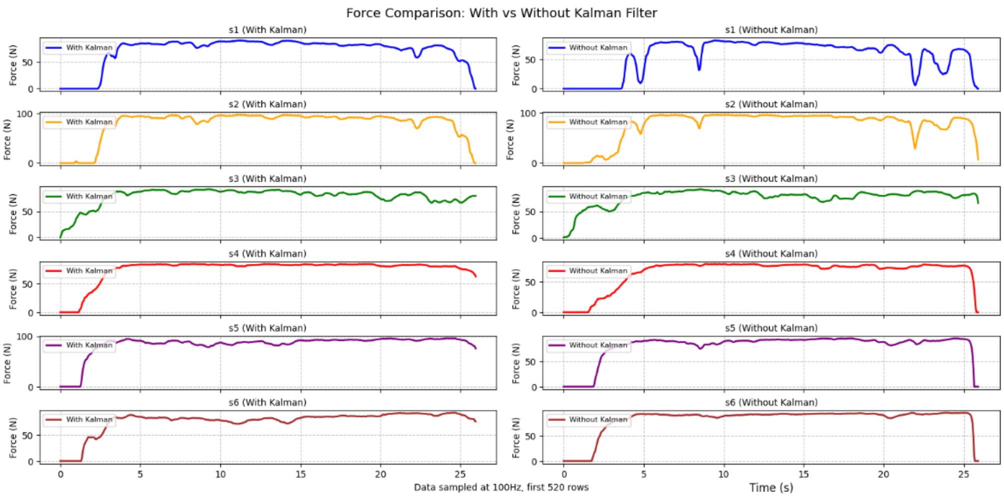

Fig. Comparison with and without Kalman filter

INTERPOLATION AND FORCE MAP VISUALIZATION

PURPOSE OF INTERPOLATION

The force sensing system developed in this project utilizes only six FSR402 sensors embedded at discrete locations in the insole. While these sensors provide localized force measurements, they are insufficient to directly capture the complete pressure distribution across the foot surface. Human foot pressure during gait is not concentrated at just a few points, but rather spread out continuously over the sole. Therefore, relying solely on the raw values from these six sensors would result in a sparse and incomplete understanding of the actual pressure pattern.

To overcome this limitation and produce a continuous and intuitive pressure map, interpolation techniques are employed. Interpolation enables the estimation of pressure values at positions where no sensor is physically present, based on the data from nearby sensors. This results in a more comprehensive visualization of the foot-ground interaction.

By applying interpolation technique, the system can simulate how pressure is likely distributed between the known sensor points, thus transforming discrete sensor data into a smooth two-dimensional pressure map. This is particularly useful in applications like gait analysis, robotic control feedback, and biomechanical monitoring, where understanding the overall pressure profile is more important than just isolated values.

In this project, Inverse Distance Weighting (IDW) is used as the interpolation method, providing a simple yet effective way to estimate unknown pressure points based on proximity-weighted sensor readings.

INVERSE DISTANCE WEIGHTING (IDW) INTERPOLATION TECHNIQUE

Inverse Distance Weighting (IDW) interpolation was employed to estimate the continuous pressure distribution across the insole surface based on discrete force measurements from the six FSR402 sensors. This deterministic method leverages the principle that the influence of a known data point decreases with distance, providing a smooth force map.

IDW assumes that the value at an unsampled point can be approximated as a weighted average of the values at known points, where the weights are inversely proportional to the distance between the points. For a grid point (x_i, y_i) the interpolated value z_i is calculated as:

$$zi = \sum_{j=1}^{n} wj.zj / \sum_{j=1}^{n} wj$$

where,

n=6(number of sensors used)

z_j=sensor force

$w_j=1/d_j^2$, is the weight assigned to sensor j

$dj = \sqrt{(xj - xi)^2 + (yj - yi)^2}$, is the Euclidean distance from the grid point to sensor j

p is the power parameter controlling the rate of distance decay.

INTERPOLATION METHODOLOGY

The interpolation process transformed the six discrete force measurements from the sensors into a continuous force map over the insole's 24x8.5 cm surface. The sensor coordinates, defined as S1 (3.7, 2.7 cm), S2 (7.0, 2.4 cm), S3 (7.0, 6.2 cm), S4 (16.5, 4.6 cm), S5 (22.0, 2.8 cm), and S6 (22.0, 6.4 cm), corresponded to the lateral forefoot, medial forefoot, midfoot, and heel regions. A 1 mm resolution grid was created using np.arange(0, 24.1, 0.1) for the x-axis and np.arange (0, 8.6, 0.1) for the y-axis, resulting in a 241x86 grid (20,726 points) represented by mesh grid arrays X and Y. The IDW interpolation was implemented in the idw_interpolation function, which calculated values at each grid point based on the inverse distance to the nearest sensors. Key constants and their roles were: Power Parameter (p) is set as 2, the inverse distance weight (w) was computed where d is the distance between a grid point and a sensor. This quadratic weighting emphasizes closer sensors, with power=2, chosen to balance smoothness and local accuracy, a common value for IDW that reduces the influence of distant points effectively. Minimum distance (dmin=0.1 cm), the distance array was clamped to a minimum of 0.1 cm using np.where(dist. < 0.1, 0.1, dist.) to avoid division by zero or undue influence from very close proximity, ensuring numerical stability and preventing singularities. Weights were normalized by their sum (w/∑w) to ensure the interpolated value (zi=∑(w×values)) remained within the force range (0-745.56 N). The function iterated over each grid point, computing distances and weights, and returned the interpolated array , which represented the estimated force distribution.

VISUALIZATION METHOD

The interpolated data is visualized using Matplotlib function in an interactive plot initialized with plt.ion () function. The plot featured the display of an image with imshow

() function with extent= [0, 24, 0, 8.5] to match the insole dimensions,
The custom colourmap is defined by LinearSegmentedColormap.from_list () with colours, breakpoints and force range as follows

Colours	**Breakpoints**	**Force range**
White	0	0-246N
Yellow	0.33	246-493N
Red	0.66	493-745.56 N
Black	1	745.56 N

Table.5.5.4.1. Visualisation Parameters

The vmin=0 and vmax=MAX_FORCE_N (745.56 N) set the color scale, with dynamic adjustment via im.set_clim() capped at the maximum observed force.
The annotation used are the sensor locations where marked with blue dots with region labels ("Forefoot," "Midfoot," "Heel") for spatial context. A colour bar with the label "Force (N)" provided a reference for the force scale.

DATA ACQUISITION AND PERFORMANCE

Serial data was received from the ESP32 at 115200 baud, with a 0.01 s timeout to handle the 100 Hz sampling rate. The script waited for a "RESET" marker before processing, then read the latest line of comma-separated smoothed forces). The max_force[0] variable tracked the highest force, capped at 745.56 N, to dynamically adjust the colour scale. The interpolated array updated the plot via im.set_array(zi), with fig.canvas.draw () and fig. canvas.flush_events() ensuring real-time rendering. Data was logged to pressure_log.csv with timestamps, and performance metrics (frame rate and processing time) were printed every second.

RESULT AND DISCUSSION

EXPERIMENTAL OUTCOME

The developed pressure mapping system aimed at estimating plantar force using a low-cost FSR402-based insole, successfully met its functional objectives. Through a systematic workflow involving sensor placement design, layered material experimentation, voltage divider-based signal acquisition, and calibration using piecewise linear models, the raw sensor data were reliably converted into force values.

To enhance the accuracy and stability of the data, Kalman filtering was applied, which significantly reduced sensor noise and yielded smoothed force outputs suitable for real-time visualization.

Further, inverse distance weighting (IDW) interpolation allowed for the generation of a full-foot force distribution map from just six sensor points. This visual representation provided meaningful insights into the load distribution during foot contact, making the system potentially useful in gait analysis for robotics .

The final prototype demonstrated satisfactory performance in capturing weight variations up to ~75 kg, with consistent outputs and real-time responsiveness at a sampling rate of 100 Hz. These outcomes affirm the feasibility of using simple resistive sensors with AI-based filtering and interpolation techniques for dynamic force monitoring applications.

INTERPRETATION OF FORCE MAP OUTPUTS

The force maps were created to visualize how force is distributed across the foot using data from six FSR402 sensors embedded in the sole. This visualization aimed to validate the system's ability to represent weight distribution patterns in real time. This can be used for getting the force feedback in the soles of Robotic gaits. For analysing the weight distribution, to check whether the force distribution is uniform, or to check the gait is stable or not, this feedback can be utilised. This was a experimental prototype, utilised to check

the feasibility of this work.

The generated maps successfully highlighted regions of high and low pressure. When weight was applied to the heel, the map showed greater intensity in the heel area, and similarly for the toe region. These responses matched known patterns of plantar force during standing, indicating that the system captured pressure zones accurately. The standing pressures was analyzed. The system showed the change in force simultaneously according to the position of the foot. Even though the setup was aimed for robotic foot feedback, due to the lack of prototype, human foots were used for force capturing. The testing was done with 6 persons.

Fig. Force Mapping System

The system displayed responsive updates to changing load conditions. When force was applied and removed, the map updated in real time, reflecting the effectiveness of the Kalman filter in stabilizing noise while preserving signal responsiveness. The maps typically showed peak force under the heel and ball of the foot, which aligns with typical human plantar force distribution. This validated both the sensor placement and the interpolation technique.

Based on the structure of foot, the force variations can be seen clearly. In the flat foot structures the peak force was seen at the midfoot and toe regions than the heel regions. To check the accuracy of the force predicted by the system data was captured by placing full load of each person on the system and calculating whole force, to check whether the total force matches with the correct weight of their body.

No.	Force(N)						Measured weight (kg)	Actual Weight (kg)
	Toe	Medial forefoot		Arch	Heel			
	S1	**S2**	**S3**	**S4**	**S5**	**S6**		
1	77.7	184.6	73.0	28.9	93.4	101.1	56.9	68
2	82.7	197.1	52.5	41.3	95.0	84.2	56.3	63
3	83.4	94.0	84.8	82	92.9	84.3	53.2	58
4	65.0	96.7	91.7	78.6	93.5	114.2	55.0	69
5	88.4	97.2	30.2	56.5	89.0	32.8	40.2	45
6	53.0	93.0	86.9	74.0	92.7	65.9	47.4	54

Table.. Summarized Mapping Data

The analysis of the collected data highlights several key strengths of the developed force mapping system. The force distribution across sensors consistently reflected expected anatomical pressure zones, with higher values recorded at the heel (S5 & S6) and forefoot (S1 & S2) compared to the arch (S3 & S4), validating the effectiveness of sensor placement. Participants such as 1, 2, and 4 exhibited typical static foot force profiles, supporting the accuracy of the system in capturing natural load patterns. In terms of weight estimation, the calculated values from the summed sensor outputs closely approximated the actual body weights, demonstrating a low average error and indicating reliable performance under static stance conditions. Notably, Participant 5, who has a flat foot condition, exhibited significantly lower force values at the arch region, which is consistent with their foot anatomy and further confirms the sensitivity of the system to individual variations. Despite such anatomical differences, the total estimated weight remained reasonably close to actual values. The system also demonstrated strong real-time responsiveness, effectively capturing variations in pressure zones across different individuals. Overall, the selected sensor layout proved robust in covering critical plantar regions, enabling balanced and informative pressure mapping without over-reliance on any single area, making the system both effective and scalable for applications in gait analysis, weight estimation, and robotic feedback systems.

Interestingly, the output also mimicked the behavior of a tactile sensor showing highly localized force responses precisely where the load was applied. This tactile-like feature makes the system not only useful for force mapping but also opens possibilities for feedback-based robotic foot design, real-time terrain interaction, and slip detection in bipedal locomotion systems.

TACTILE FEEDBACK BEHAVIOUR OBSERVED

During the static testing and real-time visualization of force mapping, an additional behaviour emerged that closely resembled the functionality of a tactile sensor. The system exhibited a clear ability to localize force zones with high spatial clarity, when force was applied to a particular region of the sole, the corresponding sensor area lit up distinctly in the force map. This was especially noticeable during fingertip press tests or when localized weights were placed directly on specific areas of the insole.

This behaviour mimics that of tactile sensing systems, which detect not only the magnitude of applied force but also the exact location of contact. The real-time force visualization dynamically adapted to changes in loading, reinforcing the system's suitability for applications such as feedback-based gait correction, robotic foot sensing, and monitoring of foot-ground interactions. The emergence of this tactile-like responsiveness highlights the effectiveness of the sensor layout, real-time data acquisition, and interpolation strategy employed.

As shown in Figure 6.3.1a, Figure 6.3.1a**,** the force map distinctly visualizes the localized force when a specific area of the insole is pressed. This emergent behaviour expands the utility of the system beyond simple force estimation, showcasing its potential as a low-cost tactile feedback mechanism for robotic and biomedical applications involving adaptive locomotion and terrain interaction.

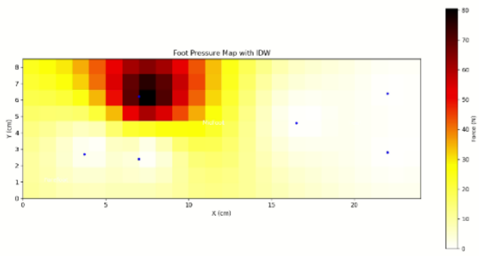

Fig. Tactile feedback 1

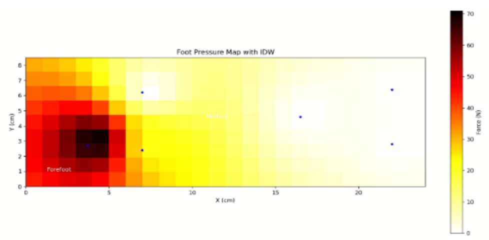

Fig. Tactile feedback 2